

Polarization dependent spontaneous-emission rate of single quantum dots in photonic crystal membranes

Q. Wang,^{1, a)} S. Stobbe,¹ H. Thyrrestup,¹ H. Hofmann,² M. Kamp,² T. Schlereth,² S. Höfling,² and P. Lodahl^{1, b)}

¹⁾DTU Fotonik, Department of Photonics Engineering, Technical University of Denmark, Ørsted Plads 343, DK-2800 Kgs. Lyngby, Denmark.

²⁾Technische Physik, Universität Würzburg, Am Hubland, D-97074 Würzburg, Germany.

(Dated: 22 December 2009)

We have measured the variation of the spontaneous emission rate with polarization for self-assembled single quantum dots in two-dimensional photonic crystal membranes. We observe a maximum anisotropy factor of 6 between the decay rates of the two bright exciton states. This large anisotropy is attributed to the substantially different projected local density of optical states for differently oriented dipoles in the photonic crystal.

PACS numbers: 78.47.da, 78.55.Cr, 78.67.Hc

Keywords: quantum dot, photonic crystal, time-resolved measurement, spontaneous emission

In the past few decades, there has been considerable interest in applying photonic crystals (PCs) for controlling the spontaneous emission (SE) of embedded emitters, which may find applications in diverse areas such as quantum information science, efficient lasers and LEDs, and for energy harvesting. Originally proposed by Yablonovitch in 1987¹, the experimental progress has been delayed due to the lack of sufficiently high quality emitters and PCs. The first experimental demonstrations of spontaneous emission control have appeared within the last five years using colloidal quantum dots or dye molecules in 3D opal PCs^{2,3,4} and self-assembled quantum dots (QDs) or quantum wells in 2D photonic crystal membranes (PCMs)^{5,6,7,8}. The latter technology has proven very successful due to the excellent optical properties of self-assembled QDs⁹, the ability to optically address single QDs⁷, and the strongly modified optical local density of states (LDOS) in PCMs¹⁰. Recently it was theoretically proposed that the spontaneous emission (SE) rate in a PC can be highly anisotropic depending on the orientation of the transition dipole moment of the emitter¹¹, which may be employed to enhance effects of quantum interference between the two radiating states¹² of relevance for quantum information applications. Here we experimentally demonstrate such a pronounced anisotropy by carrying out time- and polarization-resolved spontaneous emission measurements on a single QD addressing two orthogonally polarized bright exciton states. In this process, we probe the anisotropy of the vacuum electromagnetic field in the PCMs, which was not addressed experimentally previously.

When optically exciting a QD, choosing the sample growth direction [001] as the quantization axis (z) for

angular momentum, one lifts an electron ($S_{e,z} = \pm\frac{1}{2}$) to the conduction band leaving a heavy hole ($J_{h,z} = \pm\frac{3}{2}$) in the valence band, which can form four possible exciton states ($|h, e\rangle$): $|\frac{3}{2}, -\frac{1}{2}\rangle$, $|\frac{3}{2}, \frac{1}{2}\rangle$, $|\frac{1}{2}, \frac{1}{2}\rangle$, $|\frac{1}{2}, -\frac{1}{2}\rangle$. We note that the light holes ($J_{h,z} = \pm\frac{1}{2}$) can be neglected as the degeneracy of the light and heavy holes is lifted by the strain causing the QDs¹³. The four exciton states are categorized into two groups according to the values of their total angular momentum: bright states ($J_z = \pm 1$) and dark states ($J_z = \pm 2$), where only the bright states are optically active. Due to the reduced symmetry of self-assembled QDs and anisotropic exchange interactions, the two bright states are separated in energy (typically 0-30 μeV)¹⁴ and usually denoted as X or Y states according to their dipole orientations ($[110]$ or $[\bar{1}\bar{1}0]$). The QD spontaneous emission decay curves are in general bi-exponential, where the fast component, which is considered here, is due to recombination of the bright exciton transitions while the slow component is due to dark state recombination mediated by spin-flip processes¹⁵. Polarization resolved spontaneous-emission measurements enable addressing each of the orthogonally polarized bright exciton states individually and thereby to probe the anisotropy of the vacuum electromagnetic field in the PCM. We quantify the polarization dependence by defining the anisotropy factor $\eta^\gamma \equiv \frac{\gamma_X}{\gamma_Y}$, where γ_X (γ_Y) represents the decay rate of the X (Y) states.

The schematic of our experimental setup is illustrated in Fig. 1. The sample is a GaAs PCM with a layer of self-assembled InAs QDs of density $250 \mu\text{m}^{-2}$ embedded in the center of the membrane, see Fig. 1. It is mounted in a closed-cycle cryostat at a temperature of 10 K and excited from the top by a pulsed diode laser at 780 nm (1.590 eV, which is above the bandgap of GaAs) and a repetition rate of 20 MHz. The photoluminescence (PL) is collected through a lens (NA = 0.65), sent to a monochromator, and arrives either at a CCD camera for recording emission spectra or a silicon avalanche pho-

^{a)}Electronic mail: qinw@fotonik.dtu.dk

^{b)}Electronic mail: pello@fotonik.dtu.dk

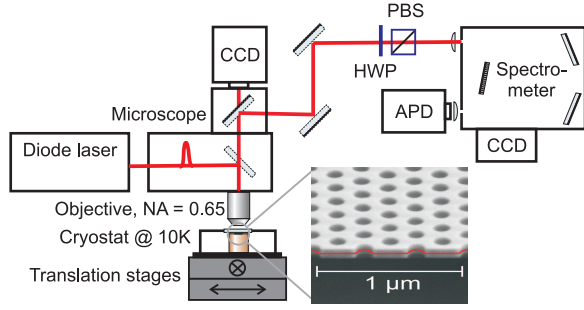


FIG. 1. (Color online) The schematic of the experimental setup. CCD: charge coupled device camera; APD: avalanche photodiode detector; HWP: half-wave plate; PBS: polarization beam-splitter. The inset shows a scanning electron micrograph of the sample, in which a layer of self-assembled InAs QDs (red color) is embedded in the center of a GaAs PCM.

todiode for the time-resolved measurements. In order to facilitate polarization resolved measurements, a polarizer consisting of a half-wave plate and a polarization beam-splitter is placed before the monochromator. The excitation intensity used in the measurements is about 300 mW/cm^2 , which is below the exciton saturation level so that only photon emission from the ground state is observed. The ground state emission wavelength is centered at 950 nm (1.305 eV) with an inhomogeneous broadening of 70 meV . The resolution of the monochromator is about $120 \text{ } \mu\text{eV}$, which is larger than the energy splitting between the two bright states. However, they can still be separated by their different polarization.

During our experiments, we investigated about 30 different QDs positioned in 7 different PCMs, with the lattice parameters ranging from 260 nm to 320 nm . For the sake of exploiting a pronounced 2D PC bandgap effect, we chose QDs in PCMs with $r/a = 0.30$, where r is the radius of the air holes and a is the lattice constant. For comparison, we also measured decay curves of 4 QDs positioned outside the PCMs. For each QD, the PL was projected onto different polarization directions by changing the orientation of the half-wave plate before the monochromator.

Fig. 2(a) shows the PL spectrum of single QDs inside a PCM by recording either horizontal (H) or vertical (V) polarizations. The spectrum is composed of sharp emission lines originating from single QDs with linewidths limited by the resolution of the spectrometer, as indicated by the shaded area in Fig. 2(a). Fig. 2(b) displays typical decay curves for two QDs, where QD A is inside a PCM, and QD B is in the unpatterned substrate while being close in emission energy to QD A. Three decay curves for QD A are displayed corresponding to different polarization components 0° (i.e. H), 70° , and 90° (i.e. V). We clearly observe that the SE rate is strongly dependent on polarization illustrating that X and Y bright excitons decay significantly different in the PCM due to the anisotropic vacuum fluctuations experienced by the

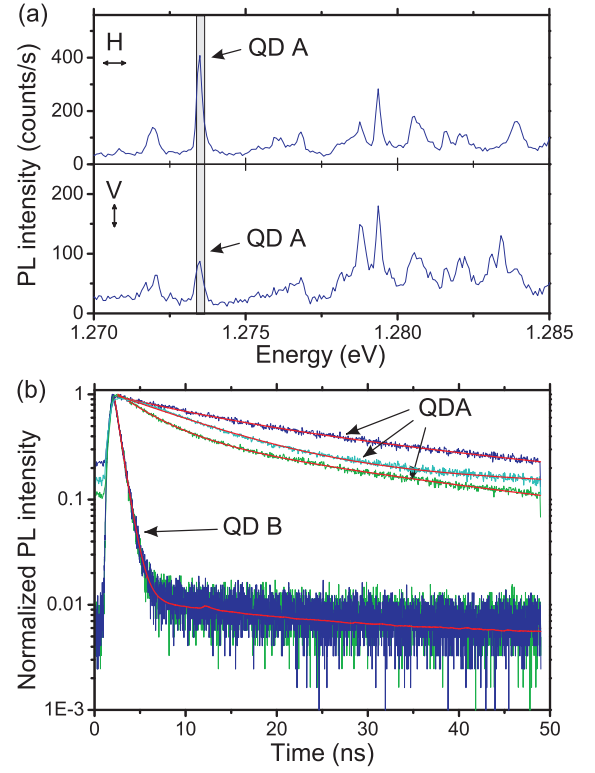


FIG. 2. (Color online) (a). PL spectra for QDs positioned in a PCM ($a = 320 \text{ nm}$) measured at H or V polarizations displaying single QD lines. The shaded area represents the resolution of the spectrometer. (b). Three decay curves for QD A (inside PCM, emission energy 1.274 eV) corresponding to 0° (blue, upper curve), 70° (cyan, middle curve) or 90° (green, lower curve) polarization. Also shown are two decay curves for QD B (outside PCM, emission energy 1.267 eV) for 0° (blue curve) and 90° (green curve) polarizations that are almost on top of each other. The red lines are bi-exponential fits to the decay curves.

QD. For comparison, no such anisotropy is observed in the reference measurements on QD B. The SE rate is furthermore found to be strongly inhibited in the PCM with the inhibition factors differing for X and Y. By comparing QD A and B we derive an inhibition factor of 15.8 for the X state and 6.5 for the Y state.

The PL intensity and decay rate obtained when probing different polarizations for QD A are presented in Fig. 3. Polarizations H and V correspond to probing the two orthogonally polarized bright states X and Y, while intermediate directions probe a combination of the two bright states. Note that this implies that only in the former case are the decay curves strictly bi-exponential functions. However this model turns out to model the decay curves rather well also for intermediate polarization settings, and the goodness-of-fit (χ^2) varying between 1.0 and 1.4 is found for the complete data set. The PL intensity shows a maximum (minimum) value at H (V) polarization, which is opposite to the decay rate. This is

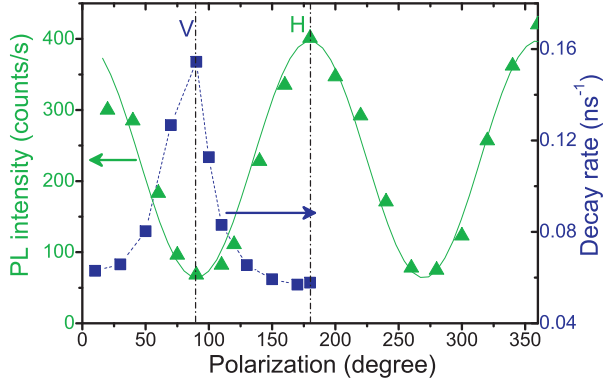


FIG. 3. (Color online) PL intensities and decay rates versus polarization for QD A. The triangular points (square points) are experimental results for intensities (decay rates). The solid line is the fitted result with a cosine function, and the dashed line is a guide to the eye.

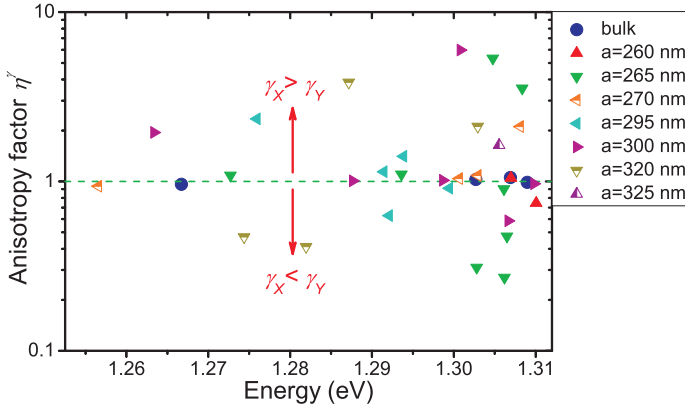


FIG. 4. (Color online) Measured anisotropy factor of decay rates between X and Y states. The triangular points represent QDs inside PCMs (with 7 different lattice parameters), the circular points represent QDs outside PCMs, and the dashed horizontal line separates regions $\gamma_X > \gamma_Y$ and $\gamma_X < \gamma_Y$.

expected since a strong suppression of the decay rate in the plane of the PCM results in a high emission vertically out of the membrane due to energy redistribution⁵. The PL intensity variation with polarization θ is observed to follow the simple relation $I = \frac{I_X + I_Y}{2} + \frac{I_X - I_Y}{2} \cos(2\theta)$, where I_X and I_Y are the intensities of the X and Y exciton states, respectively, see Fig. 3. This can be easily understood as the result of applying polarization projection measurements on two orthogonal states.

Fig. 4 shows the anisotropy factor of decay rates for all the measured QDs measured on PCMs with various values of the lattice constant. Note that in all measurements

presented in the present manuscript the QD emission was within the 2D photonic bandgap of the PCMs¹⁰. Large variations are observed between the individual QDs in the PCM with a maximum value of about 6. This directly demonstrates the large anisotropy of the vacuum electromagnetic field in a PC that was theoretically proposed in Ref.¹¹. This anisotropy gives rise to substantial differences in the projected LDOS leading to the different decay dynamics of X and Y exciton states. For comparison, reference QDs in a bulk substrate showed no anisotropy in the decay rates for the two orthogonally polarized states.

To conclude, we have systematically measured the polarization dependent SE rate for self-assembled single QDs inside PCMs and obtained a maximum anisotropy factor of decay rate between the X and Y states of 6. Our measurement results demonstrate the large anisotropy of the vacuum electromagnetic field inside PCMs^{10,11}, which is a crucial condition for achieving quantum interference between two closely lying energy levels¹² that could enable demonstration of fascinating phenomena, such as lasing without inversion¹⁶ or quantum beats¹⁷. Therefore, our experiment is not only vital in realizing complete control of the SE of single QDs with PCs, but also enables fundamental quantum optics experiments with practical systems.

ACKNOWLEDGMENTS

We thank T. Lund-Hansen and M. L. Andersen for help during the experiment, and we gratefully acknowledge financial supports from the Danish Research Council (FTP grant 274-07-0459 and FTP/FNU grant 272-09-0159).

- [1] E. Yablonovitch, Phys. Rev. Lett. **58**, 2059 (1987).
- [2] P. Lodahl *et al.*, Nature **430**, 654 (2004).
- [3] I. S. Nikolaev, P. Lodahl, A. F. Koenderink, and W. L. Vos, Phys. Rev. B **75**, 115302 (2007).
- [4] I. S. Nikolaev, P. Lodahl, and W. L. Vos, J. Phys. Chem. C **112**, 7250 (2008).
- [5] M. Fujita *et al.*, Science **308**, 1296 (2005).
- [6] M. Kaniber *et al.*, Appl. Phys. Lett. **91**, 061106 (2007).
- [7] M. Kaniber *et al.*, Phys. Rev. B **77**, 073312 (2008).
- [8] B. Julsgaard *et al.*, Appl. Phys. Lett. **93**, 094102 (2008).
- [9] J. Johansen *et al.*, Physical Review B **77**, 073303 (2008).
- [10] A. F. Koenderink, M. Kafesaki, C. M. Soukoulis and V. Sandoghdar, J. Opt. Soc. Am. B **23**, 6 (2006).
- [11] W. L. Vos, A. F. Koenderink and I. S. Nikolaev, Phys. Rev. A **80**, 053802 (2009).
- [12] G. S. Agarwal, Phys. Rev. Lett. **84**, 5500 (2000).
- [13] M. Bayer *et al.*, Phys. Rev. B **65**, 195315 (2002).
- [14] R. M. Stevenson *et al.*, Phys. Rev. B **73**, 033306 (2006).
- [15] J. Johansen, B. Julsgaard, S. Stobbe, J. M. Hvam, P. Lodahl, arXiv:0905.4493.
- [16] A. Imamoglu, Phys. Rev. A **40**, R2835 (1989).
- [17] O. Kocharovskaya *et al.*, Found. Phys. **28**, 561 (1998).